

AEM Surveys Applied for Iron Formation Mapping: A Proxy for Iron Ore Exploration

Marco Antonio Couto Junior¹, Dionisio Uendro Carlos¹ and Raphael Fernandes Prieto¹
¹VALE S.A. (Ferrous Exploration Team)

SUMMARY

The use of Airborne Electromagnetic data in iron ore exploration is yet not a standard approach to map mineralized iron formations and their relations with the host rocks. However, initial results conducted by VALE's ferrous geophysics team have been demonstrating promising on the potential use of such methodology. Both time and frequency domain data demonstrated a clear spatial correlation of strong resistors with the position of known mineralized iron formation layers in the Serra Sul region, Carajás Mineral Province, Brazil. This paper presents the first results and discusses the future challenges regarding the use of this type of data.

Keywords: AEM, Mineral Exploration, Iron Ore

INTRODUCTION

In mineral exploration, the Airborne Electromagnetic Methods (AEM) have become the benchmark in the geophysicist's utility belt to map highly conductive targets related to base metals mineralization. The variable set of AEM methods has demonstrated its effectiveness in mapping conductive massive sulfides related to all sorts of deposit styles for base metals, like porphyries, volcanogenic-hosted-massive sulfides (VHMS), orogenic gold, iron-oxide-copper-gold (IOCG), among others, for more than five decades - [Okada \(2022\)](#) and [Ley-Cooper & Viezzoli \(2017\)](#). However, concerning the exploration of iron ore with supergene alteration genesis, the method is still not a standard approach, with very scarce literature related to it, limiting it to a few case studies in the Hamersley Basin in Australia, as presented by [Neroni et al. \(2016\)](#) and [Flis et al. \(1998\)](#), although it demonstrated its significant value in mapping mineralized iron formations.

VALE's ferrous geophysics team in Brazil has been conducting a set of experiments regarding the use of AEM data to delineate the mineralized iron formation layers in the Carajás Mineral Province (CMP) and in the Iron Quadrangle Mineral Province (IQMP), Northern and Southeast Brazil, respectively. The early experiments started in 2020, with the execution of more than 18,000 km of RESOLVE surveys, a frequency domain electromagnetic (FDEM) airborne system. Most of these surveys focused on geotechnical and hydrogeological studies, but a few blocks were conducted over mineralized iron formation in both CMP and IQMP. These surveys demonstrated important resistive anomalies related to the iron ore formations.

Particularly, in the CMP, these resistive anomalies clearly present a strong spatial correlation with known mineralized iron formation in the Serra Sul iron mine. The comparison of these results with historical GEOTEM surveys, a

transient electromagnetic (TEM) airborne system, showed a strong correlation of known mineralized iron formation with resistive zones on the district scale, supported by petrophysical data in key lithotypes related to the mineralization. These results supported and encouraged the execution of more than 7,000 km of Helitem surveys in the CMP, focusing on key iron ore targets, with promising results to offer more detailed resistivity mapping compared to the historical data and a significant complement to the standard approach in iron ore mapping, i.e., Airborne Gravity Gradiometry (AGG) and Airborne Magnetics (AMAG). This paper presents the Serra Sul results of these experiments conducted by the VALE ferrous team so far and points out future directions in AEM research for iron ore mapping.

AREA OF STUDY

The study area is in the Serra Sul region in the CMP, Pará State, Brazil, particularly in the S11D mine and the S16 target (Figure 1a). In this area, the iron formation is composed by compact jaspelites layers from the Carajás Formation at the bottom of the sequence, followed by friable hematite towards to the top of the layer, due to the supergene alteration process - [Silva & Costa \(2020\)](#). On the top of it, iron crust occurs as the product of the foremost supergene alteration process within the iron formation. The host rocks for the iron formation are composed by metabasalts from the Igarapé-Cigarra and Parauapebas Formations to the North and South, respectively (Figure 2b).

MATERIAL AND METHODS

The AEM Surveys

The AEM surveys studied in this work are composed of GEOTEM, Helitem, and RESOLVE data. The basic system information and flight specs are presented in Tables 1 and 2 for the airborne TEM and FDEM systems, respectively. All surveys present the magnetic data acquired jointly, but only the AEM data will be discussed here.

Specification	GEOTEM	Helitem
Base Freq. (Hz)	90	30
Waveform Type	Half-sine	Rectangular
Pulse Width (ms)	2.08	8.89
Dipole Moment (NIA)	418,000	461,000
No. of Channels	20	25
Terrain Clearance (m)	120	50-60
Line Spacing (m)	250	100
Line Direction	N-S	N-S

Table 1: Specifications for the airborne TEM systems: GEOTEM and Helitem.

Dip. Moment (Am2)	Coil Orient.	Freq.
359	HCP	400 Hz
187	HCP	1.8 kHz
150	VCA	3.3 kHz
72	HCP	8.2 kHz
49	HCP	40 kHz
17	HCP	140 kHz

Table 2: Specifications for the RESOLVE system. HCP: horizontal coplanar and VCA: vertical coaxial coil orientations. The survey was conducted with 50 m line spacing, 63 m terrain clearance and N-S orientation. For further details about the RESOLVE system, check [Geosci.xyz](#) documentation.

Data Processing and Modeling Approach

The modeling approach was based on different commercial inversion solutions for each type of AEM data: FDEM and TEM.

The RESOLVE data were processed by the contractor, which focused on the removal of any anthropogenic and/or coupling effects within the data. No additional processing was applied. The inversion was conducted using the 1D VOXI-EM suite available in Sequent Oasis Montaj software, which solves for the electrical conductivity using the approach from [Ellis \(1999\)](#) and minimizes the objective function using the Tikhonov minimum gradient regularizer. We followed all the recommendations presented in the [VOXI-EM Sequent's documentation](#), running uncon-

strained inversions. The mesh was defined with regular cells with 1/4 line spacing horizontal dimensions and a 5 m vertical dimension. The estimated error was defined as the data relative error noise floor for each RESOLVE's frequency, based on the noise level measured during the altitude flights (we used 5% or 10% depending on the frequency).

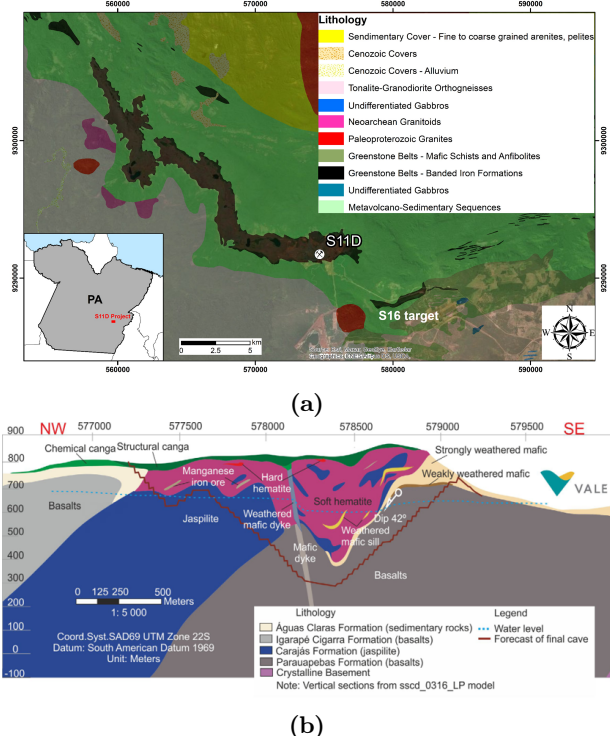


Figure 1: (a) Serra Sul region in the CMP. The S11D mine and S16 target are indicated. (b) NE-SW schematic section in the S11D region - figure from [Silva & Costa \(2020\)](#).

The GEOTEM data were not processed or modeled due to the incompleteness of information regarding this historical data; they were only used for dB/dt and apparent conductance maps for interpretation. Nevertheless, the Helitem data were processed using the AGS Workbench suite, with the application of automatic processing and further manual/visual refinement, following a similar approach presented in [Auken et al. \(2009\)](#). The automatic processing focused on running moving averages for each time regime (narrow and wide time windows for early and late times, respectively) and on removing steep decays to cull out any induced polarization (IP) effects present in the data. Additionally, the noise floor estimation was conducted based on the data standard deviation, and it was considered to remove noisy data in the late times.

The Helitem data were finally inverted using the Spatial-Constrained-Inversion (SCI) technique - [Viezzoli et al. \(2008\)](#), based on the AarhusInv code workflow presented in

Auken et al. (2015), implemented in the AGS Workbench, which applies a modified Marquardt optimization process. This technique is based on a 1D inversion approach, but with spatial constraints along and between the flight lines, aiming to recover a quasi-3D model. In this work, the 1D models were smoothly discretized into 25 layers, with a 5 m thickness for the first layer, logarithmically increasing downwards until a 500 m depth. The smooth model assumes that the layer resistivities can vary freely through the model with fixed thicknesses. The starting resistivity model considered a 500 $\Omega \cdot m$ semi-space, constrained with a factor of 1.3, meaning that 30% variations from the initial model were allowed.

RESULTS

The analysis started in the S11D mine with the RESOLVE survey data in this area (Figure 2c). The RESOLVE inversion recovered a strong resistive body (conductivity values smaller than 10^{-5} mS/m) with a clear spatial association with the position of known iron formation layers in the D body in the S11D mine, as shown in Figure 2a, suggesting its continuation into the C body (the contact zone is indicated in Figure 2a). In fact, the strong resistive anomaly spatially agrees quite well in depth with the known undivided iron formation (which includes all types of iron bodies, mainly: jaspelite, friable hematites, and iron crust). The petrophysical data from the borehole geophysics in the S11D mine (not shown in this paper) confirmed this resistivity contrast between the undivided iron formation (resistivity values greater than $1000 \Omega \cdot m$) from the Carajás Formation and their host rocks composed by the weathered altered mafic units from the Parauapebas and Igarapé-Cigarra Formations (resistivity values smaller than $500 \Omega \cdot m$).

Regionally, the GEOTEM apparent conductance demonstrated this continuity to the whole S11 body, towards NW (Figure 2c), with conductance values around zero.

As mentioned earlier, these results motivated the execution of newer Helitem surveys in the Serra Sul region. Although these surveys did not cover the same area as the RESOLVE survey, they covered the S16 target, a key mineralization for the Serra Sul exploration program. The processed and modeled data using the SCI approach are presented in Figure 4. The raw data showed a strong resistive domain over the plateau of the iron formation (an amplitude drop in the dB/dt data), and the suggestion of a strong IP effect in the region of the mafic units to the southern portion of the area, indicated by the late times negative values. The IP effect was not addressed in this work yet, as the real resistivity parameterization was used. The SCI model indicates the continuity of the resistive anomaly related to the mineralized iron formation layer to the Northern region of the plateau, as indicated by the lithological borehole information in Figure 3b.

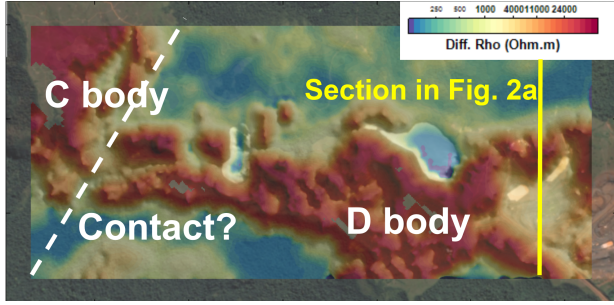
Spatially, the Helitem data present a strong resistor (values greater than $1000 \Omega \cdot m$) associated with the iron formation plateau in the S16 target region, suggesting its continuity towards the Eastern portion of the area. In comparison with the conductance information recovered from the regional GEOTEM data in the same area, a significant improvement in the resistivity model spatial resolution can be noted.

DISCUSSION AND NEXT STEPS

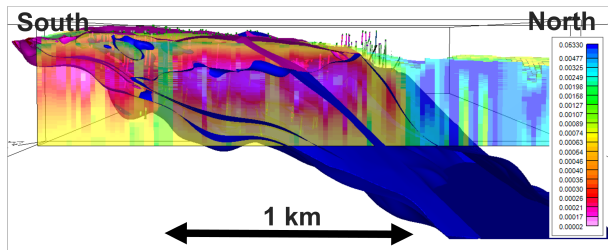
The AEM data in the Serra Sul area proved to be useful in mapping the strong resistor associated with known mineralized iron formation layers. These resistors are also strongly correlated with AGG and AMAG data (not shown in this paper), which are the standard geophysical approaches for iron ore exploration in VALE's deposits in Brazil. Although this is not discussed in this paper, the AEM data provided greater spatial resolution in comparison to these other two methodologies, becoming an additional geophysical tool for iron ore exploration.

However, a set of challenges still remains regarding the optimal use of AEM data. The first is properly addressing data distortion due to natural effects related to the EM fields and their relationship with subsurface mineral content, such as the IP and the superparamagnetic effects. The Helitem and RESOLVE data clearly highlight the significance of these distortions in the iron ore context, showing negative late-time transients and negative signals at the lower frequencies (for the FDEM data, not shown in this paper), respectively. Properly addressing these effects will allow to recover more reliable resistivity models and achieve better geological interpretation.

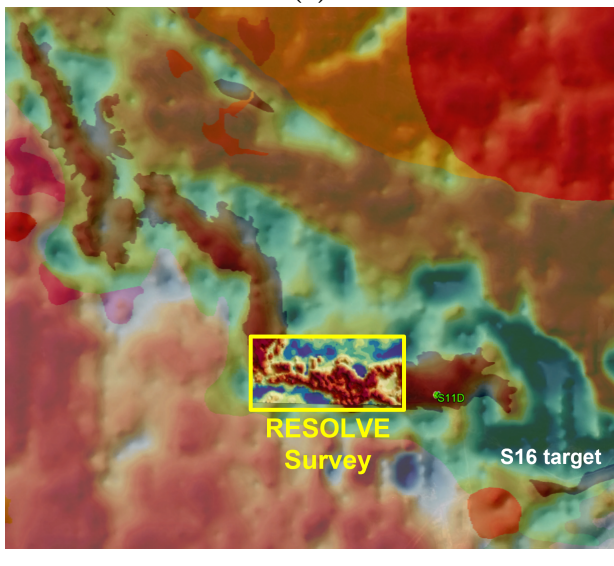
The second challenge concerns the best way to integrate the AEM with AGG and AMAG data seeking to improve their interpretation, specially for non-geophysicists fellow colleagues. VALE's ferrous geophysics team is currently addressing this topic in collaboration with [MIRA Geoscience](#), developing an AEM processing suite based on Auken et al. (2009) and joint 3D inversions of all these three methodologies. The project is ongoing and the first results applying the cross-gradient approach for joint inversions demonstrated promising results to improve each methodology inversion. Our team is also currently exploring Artificial Intelligence approaches, working on the creation of Machine Learning models as lithological predictors, seeking to improve the use of geophysical data for the geological framework modeling, a key step in the resource estimation. The initial results (not presented in this paper) are very promising and they should be improved with better data processing and modeling.



(a)



(b)



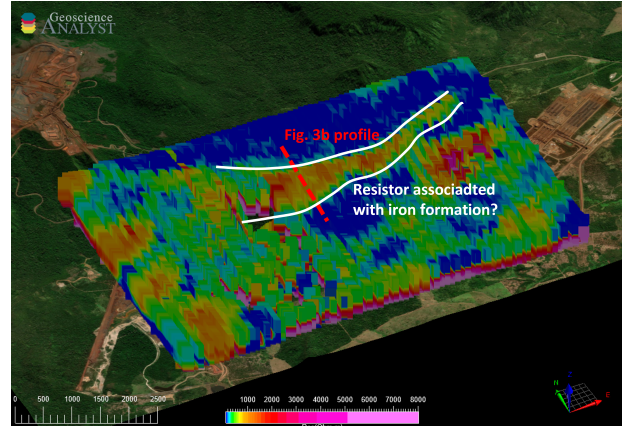
(c)

Figure 2: (a) RESOLVE survey area in S11D mine, with the indication of mineralized bodies C and D over the resistivity map for this area. (b) RESOLVE conductivity model (in mS/m) for the profile indicated in Figure 2a. (c) GEOTEM apparent conductance map over the geological map (50% transparency) in the Serra Sul area, including all mineralized bodies in the S11 deposit and the S16 target, and the RESOLVE survey area. Red and blue colors mean lower and higher conductance domains.

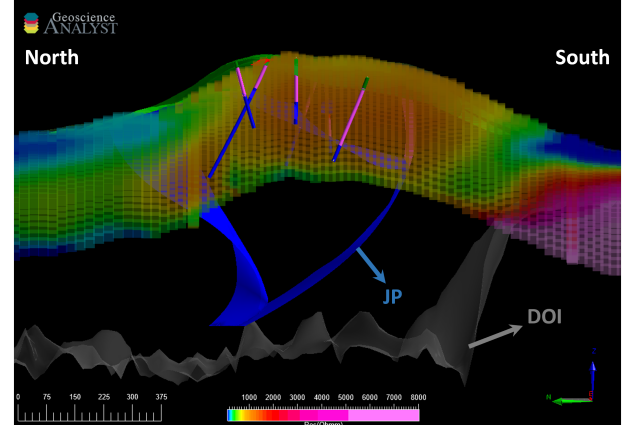
CONCLUSION

The Serra Sul case demonstrated that the AEM data is an useful tool in the geophysicist's options to be applied

in iron ore exploration. The mineralized iron formations clearly present an important spatial correlation with strong resistors in this geological environment, allowing to define their contact within the mafic host rocks. However, proper data processing and modeling routines, along with optimal data integration with other geophysical methodologies are the current challenges on the use of this data. VALE geophysics team already started to investigate these problems, bringing exciting discussion in the near future.



(a)



(b)

Figure 3: (a) Helitem SCI model (resistivity) over the S16 target. (b) SCI section indicated in Figure 3a. The lithological borehole data and the geological models are presented in the section. The lithological color code follows the one in Figure 2b.

ACKNOWLEDGMENTS

The authors would like to thank VALE S.A. for the permission of this publication. They also thank Sequent and AGS for the Workbench trial license used to process and run the inversions of the Helitem data.

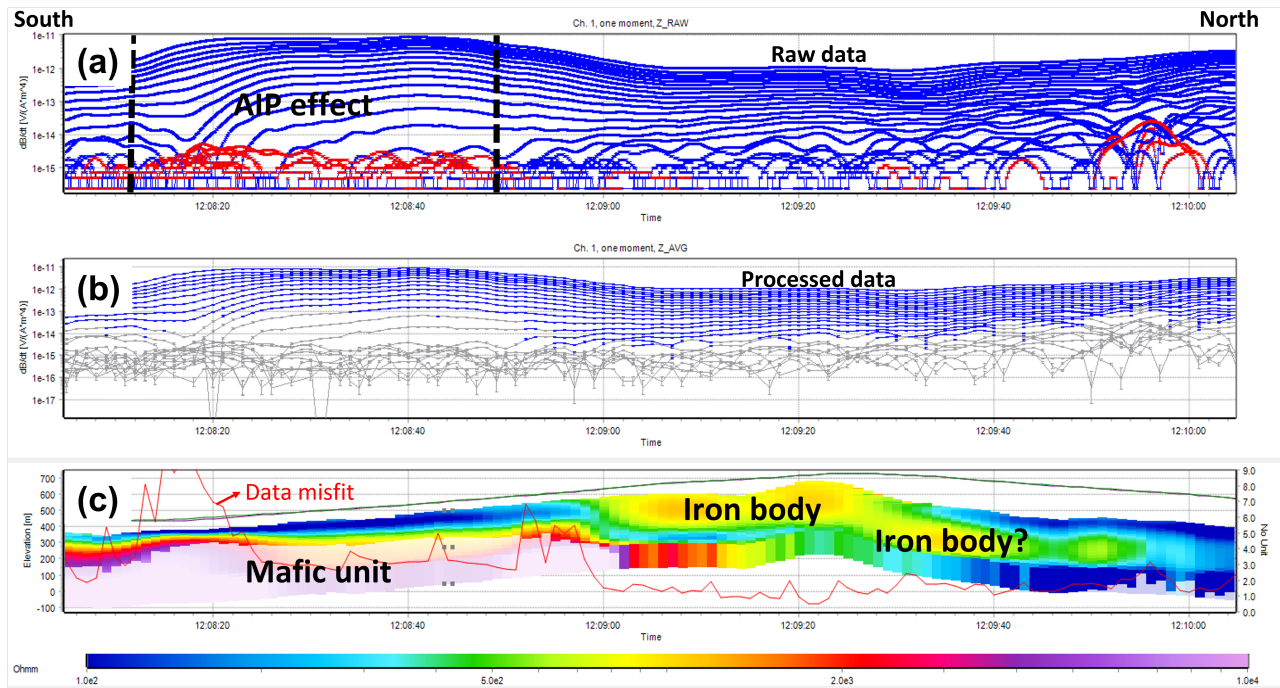


Figure 4: Helitem processing and SCI model over the S16 target with geological interpreted. (a) Raw data. (b) Processed data. (c) SCI resistivity section. This section refers to the one indicated in Figure 3a.

REFERENCES

- Auken, E., Christiansen, A. V., Kirkegaard, C., Fiandaca, G., Schamper, C., Behroozmand, A. A., et al. (2015). An overview of a highly versatile forward and stable inverse algorithm for airborne, ground-based and borehole electromagnetic and electric data. *Exploration Geophysics*, 46(3), 223-235.
- Auken, E., Christiansen, A. V., Westergaard, J. H., Kirkegaard, C., Foged, N., & Viezzoli, A. (2009). An integrated processing scheme for high-resolution airborne electromagnetic surveys, the SkyTEM system. *Exploration Geophysics*, 40(2), 184-192.
- Ellis, R. G. (1999). Smooth 3D inversion of airborne transient electro-magnetic data using the TFQMR-FFT fast integral equation method. In *Proceedings of the Second International Symposium on Three-Dimensional Electromagnetics*. The University of Utah.
- Flis, M., Hawke, P., & McMillan, A. (1998). The application of multifrequency airborne electromagnetics to iron ore exploration. *Exploration Geophysics*, 29(1-2), 254-258.
- Ley-Cooper, A., & Viezzoli, A. (2017). Airborne EM: An Important Exploration Method for Revealing Geological Insights into the Subsurface. In Y. Berbers & W. Zwaenepoel (Eds.), *Proceedings of Exploration 17: Sixth Decennial International Conference on Mineral Exploration*. Decennial Minerals Exploration Conferences.
- Neroni, R., Murray, R., & Kepert, D. (2016). Application of the airborne electromagnetic method for Banded Iron-Formation mapping in the Hamersley Province, Western Australia. *ASEG Extended Abstracts*, 2016(1), 1-8.
- Okada, K. (2022). Breakthrough technologies for mineral exploration. *Mineral Economics*, 35, 429-454.
- Silva, A. C. S., & Costa, M. L. (2020). Genesis of the ‘soft’ iron ore at S11D Deposit, in Carajás, Amazon Region, Brazil. *Brazilian Journal of Geology*, 50(1).
- Viezzoli, A., Christiansen, A. V., Auken, E., & Sørensen, K. (2008). Quasi-3D modeling of airborne TEM data by spatially constrained inversion. *Geophysics*, 73(3), F105-F113.